Fermilab muon g-2 experiment

Tim Gorringe[1,a] on behalf of the Fermilab muon g-2 collaboration.

[1] *Department of Physics and Astronomy, University of Kentucky, Lexington, KY, 40502, USA*

Abstract. The Fermilab muon g-2 experiment will measure the muon anomalous magnetic moment a_μ to 140 ppb – a four-fold improvement over the earlier Brookhaven experiment. The measurement of a_μ is well known as a unique test of the standard model with broad sensitivity to new interactions, particles and phenomena. The goal of 140 ppb is commensurate with ongoing improvements in the SM prediction of the anomalous moment and addresses the longstanding 3.5σ discrepancy between the BNL result and the SM prediction. In this article I discuss the physics motivation and experimental technique for measuring a_μ, and the current status and the future work for the project.

1 Introduction

These are interesting times in physics. With dark matter and dark energy being thought to comprise about 95% of the universe's mass, the standard model of particle physics seems astonishingly incomplete. Unfortunately – despite enormous efforts at high energy colliders, in deep underground searches, and elsewhere – no definitive evidence of new interactions, particles or phenomena has been found in any sub-atomic experiments.

It is nearly 20 years ago that the BNL 821 collaboration reported its now celebrated 540 ppb measurement [1] of the muon anomalous magnetic moment, a_μ. The BNL result and SM prediction were found to differ by roughly 3.5 σ. This discrepancy has survived experimental and theoretical scrutiny and today remains the most tantalizing and persistent hint from sub-atomic experiments of physics beyond the standard model.

In this article I will describe the new Fermilab muon g-2 experiment [2] – the direct descendant of BNL 821. The Fermilab experiment is designed to determine the muon anomaly a_μ to an unprecedented 140 parts-per-billion precision. Such precision will provide a unique test of the standard model and offer a broad sensitivity to new physics that complements other efforts at the energy, intensity and cosmic frontiers. Most importantly, it addresses the longstanding discrepancy between the SM prediction and the BNL experiment and – whether it confirms or refutes this discrepancy – will surely have broad impact and enduring value in nuclear, particle and astrophysics.

In what follows I offer an experimentalist's perspective on the physics interest, discuss the techniques exploited in the anomaly's measurement, and provide the current status and future work of the project.

Note an alternative measurement of the muon anomaly – employing a novel source of polarized muons and different approach to muon storage – is being pursued by the J-PARC E34 experiment [3]. It is described elsewhere in the conference proceedings.

[a] e-mail: gorringe@pa.uky.edu

2 Physics motivation

While collider experiments offer exceptional access to interactions and particles that lie within their energy range, the precision measurement of fundamental quantities offers opportunistic windows on new physics that's capable of reaching to much higher energy scales. In particular – through the subtle effects of quantum fluctuations – the muon magnetic moment is a unique portal to new phenomena at collider energies and beyond.

The muon anomaly a_μ is important because it's calculable and measurable with extraordinary precision; thereby offering both an exacting test of the standard model and a sensitive probe of any new physics (for details see Refs. [4, 5]). The BNL result [1] of

$$a_\mu^{exp} = (116\,592\,089 \pm 63) \times 10^{-11} \tag{1}$$

has been one of the most-cited measurements of the past twenty years. Despite the intense theoretical and experimental scrutiny the longstanding discrepancy between the SM prediction and the BNL result has only strengthened over the years since the experiment.

Presumably all forces of nature – both known and unknown – give contributions to a_μ. Within the standard model the muon anomaly a_μ receives contributions from QED loops involving electrons and photons, electroweak loops involving W, Z and Higgs bosons, and hadronic loops involving quarks and gluons,

$$a_\mu^{SM} = a_\mu^{QED} + a_\mu^{EW} + a_\mu^{had}. \tag{2}$$

By far the largest contribution is the famous Schwinger term $\alpha/2\pi$ involving a roughly part-per-thousand correction of the muon magnetic moment. However, the

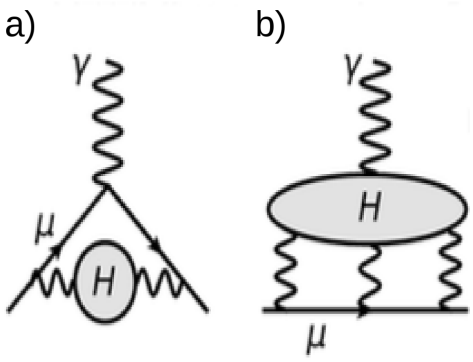

Figure 1. Feynman diagrams for a) the leading-order hadronic vacuum polarization contribution and b) the hadronic light-by-light scattering contribution.

overwhelming uncertainty in calculating a_μ^{SM} arises from hadronic vacuum fluctuations and how quarks and gluons dress the muon magnetic moment (see Fig. 1). As is discussed elsewhere in these conference proceeding, the most recent updates for the leading-order hadronic contributions $a_\mu^{had:LO}$ of 6922 ± 25, 6926 ± 33 and $6881 \pm 41 \times 10^{-11}$ from the Teubner *et al.*, Davier *et al.* and Jegerlehner [6–8] have lowered the uncertainties by roughly 25-50% over earlier estimates [9–11]. By comparison the uncertainties in the QED contribution, 0.08×10^{-11} [12], and the electroweak contribution, 1.0×10^{-11} [13], are completely negligible.

The largest uncertainty in the hadronic term arises from the leading-order hadronic vacuum polarization term $a_\mu^{had:LO}$. Since $a_\mu^{had:LO}$ isn't yet calculable with sufficient accuracy, its value is evaluated via dispersion relationships from an energy-weighted integral of the measured $e^+e^- \rightarrow$ hadrons cross section. The energy-weighting emphasizes the low-energy region that is dominated by the ρ and ω resonances and the $e^+e^- \rightarrow 2\pi$ channel. Recent estimates of $a_\mu^{had:LO}$ have benefited from new measurements and new analyses of e^+e^- data as well as more sophisticated treatments of the correlated systematic errors between the e^+e^- datasets. At present the uncertainty in $a_\mu^{had:LO}$ is dominated by the systematic errors in the experimental results for the various $e^-e^+ \rightarrow \pi\pi$ channel. The relevant data were obtained using initial-state radiation and energy-scan techniques and – while generally in agreement – there remains tension between BaBar data and other data at energies just above the ρ, ω resonances.

The other important contribution to the hadronic uncertainty is the hadronic light-by-light term a_μ^{hLBL}. For many years the estimation of a_μ^{hLBL} was limited to specific models of the hadronic loop in the four-photon vertex with the so-called "Glasgow consensus" $a_\mu^{hLBL} = (105 \pm 26) \times 10^{-11}$ emerging as the accepted value for the hadronic light-by-light contribution. One new approach, using lattice QCD, offers the prospect of a first-principles calculation of a_μ^{hLBL} at the 10% level. Another new approach, using dispersion relations, offers the prospect of a data-driven extraction of a_μ^{hLBL} by relating the quantity to pion form factor and $\gamma^*\gamma^* \rightarrow \pi\pi$ scattering data.

The effort to determine a_μ^{had} was discussed in great detail at this conference and represents a remarkable triumph of combined theoretical and experimental labor. Many talks spotlighted the continuing push to better quantify the hadronic corrections and associated uncertainties with theoretical tools including dispersion relations, lattice QCD, effective theories and hadronic models as well as ingenious new experimental ideas. The SM prediction for a_μ is currently known to about 400 ppb – to bring this uncertainty on par with experimental goals will need a roughly 0.2% determination of the hadronic vacuum polarization term and a roughly 10% determination of the hadronic light-by-light term.

Using the recent updates for the hadronic correction, the differences in a_μ between the BNL result and the SM prediction are $a_\mu^{exp} - a_\mu^{SM} = (288 \pm 80)$, (281 ± 73), and $(313 \pm 77) \times 10^{-11}$ [6–8]; a discrepancy of 3.6 to 4.1 σ. To set the scale – this discrepancy is roughly twice the entire contribution of electroweak effects – these effects mostly arising from one-loop diagrams involving virtual W and Z bosons.

New physics will typically make contributions to a_μ from one-loop diagrams at scales of $O(Cm_\mu^2/M^2)$ where C and M are the coupling constant and the mass scale of the new interaction. For couplings of order $O(1)$ the discrepancy would imply multi-TeV mass scales. By comparision, for electroweak-scale coupling $O(\alpha/4\pi)$ it would imply a sub-TeV mass scale and for milli-scale couplings $O(10^{-3})$ it would imply a GeV mass scale.

The anomalous magnetic moment represents a uniquely inclusive probe of new physics that nicely complements the specific sensitivities of collider experiments, underground searches, *etc*. Indeed the BNL result has major consequences for many SM extensions including extra Higgs, supersymmetric partners and dark photons, in some cases it pushing practitioners into small corners of model space. If new physics is discovered elsewhere the muon anomaly will surely play an important role in interpreting the signal. And - if new physics isn't discovered elsewhere – the anomaly is then the wide net to catch new physics.

3 Experimental technique

As mentioned, the Fermilab muon g-2 experiment [2] is designed to measure a_μ to 140 ppb precision, a goal commensurate with anticipated improvements in the present knowledge of the hadronic contributions from new e^+e^- data and theoretical advances.

The Fermilab experiment will use the same basic technique as the earlier BNL experiment. It involves injecting fills of polarized muons with magic momenta 3.094 GeV/c into the 1.54 T magnetic field of the 7.1 m radius storage ring. Within the ring the muons orbit at the cyclotron frequency ω_c and their spins rotate at the Lamor frequency ω_s. If a_μ was zero – *i.e.* muons were Dirac particles with g-factor $g \equiv 2$ – the two frequencies would be identical. However, for a non-zero anomalous magnetic moment the

Figure 2. Schematic of Fermilab muon campus showing the M1 line for 8 GeV proton delivery, the AP0 production target for pion production, the M2 / M3 lines for 3.11 GeV/c pion collection and 3.09 GeV/c muon capture, the delivery ring for separating muons, pions and protons, the M5 line for beam delivery to the g-2 experiment, and the line M4 for beam delivery to the Mu2e experiment.

two frequencies differ by $\vec{\omega_a} \equiv \vec{\omega_s} - \vec{\omega_c}$ where

$$\vec{\omega_a} = \frac{q}{m}[a_\mu \vec{B} - (a_\mu - \frac{1}{\gamma^2 - 1})\vec{\beta} \times \vec{E}/c], \qquad (3)$$

is the so-called anomalous precession frequency. At the magic momentum 3.094 GeV/c – where $\gamma = 29.3$ – the term in Eqn. 3 involving the electric field vanishes. Thus measurement of ω_a and B, and knowledge of q and m, together permit the determination of a_μ. One attractive feature of the experimental technique is the direct measurement of the anomalous part of the magnetic moment arising from vacuum fluctuations.

In practice, the experiment involves precisely measuring two frequencies; the muon anomalous precession frequency ω_a that was introduced above and a proton Lamor precession frequency ω_p for the B-field determination.

At the magic momentum the muons have a time-dilated lifetime of 64.4 μs and their spin advances about one extra turn for every thirty orbits of the storage ring. The frequency ω_a can be obtained from its sinusoidal modulation of the time distribution of the positrons emitted in the muon decays. The positrons are detected by calorimeters that are located on the inner circumference of the storage ring (the positrons have lower momenta than stored muons and spiral inwards). The origin of the ω_a-modulation is the self-analyzing nature of the muons, *i.e.* the high energy decay positrons are preferentially emitted along the muon spin direction. When the positron emission is directed along the muon orbit the Lorentz boost yields higher-energy positrons. When the positron emission is directed opposite the muon orbit the Lorentz boost yields lower-energy positrons. Consequently, the lab-frame energy of emitted positrons oscillates sinosoidally with frequency ω_a. Thus, by measuring either the integrated positron energy versus time or the high-energy positron counts versus time, the frequency ω_a is extractable.

The relevant B-field in Eqn. 3 is the magnetic field averaged over the muon beam distribution. A combination of fixed NMR probes and movable NMR probes are used to measure the proton Lamor frequency ω_p in the storage ring magnetic field. Nearly 400 fixed probes are distributed around the ring's circumference at locations either just above or just below the vacuum vessel. Additionally, 17 movable probes are mounted to a trolley that can circumnavigate the vacuum vessel interior in dedicated, beam-off, trolley runs. A special NMR probe is used for the 20 ppb absolute calibration of the entire NMR system. This system – together with accompanying measurements of the spatial distribution of the stored beam – thereby enables the determination of the beam-weighted, Lamor frequency $\overline{\omega}_p$.

From the determination of the muon's anomalous frequency, ω_a, and the proton's Lamor frequency, $\overline{\omega}_p$, the anomaly a_μ is extracted via

$$a_\mu = \frac{\omega_a/\overline{\omega}_p}{\mu_\mu/\mu_p - \omega_a/\overline{\omega}_p} \qquad (4)$$

where μ_μ/μ_p is the muon-to-proton magnetic moment ratio. The quantity μ_μ/μ_p is needed as the frequency ω_a is proportional to the muon's anomalous magnetic moment whereas the frequency $\overline{\omega}_p$ is proportional to the proton's total magnetic moment. Fortunately, the ratio μ_μ/μ_p is precisely known from muonium spectroscopy – it having previously been measured at LAMPF to a 26 ppb precision and is currently being remeasured at J-PARC with a 10 ppb goal (see Ref. [5]).

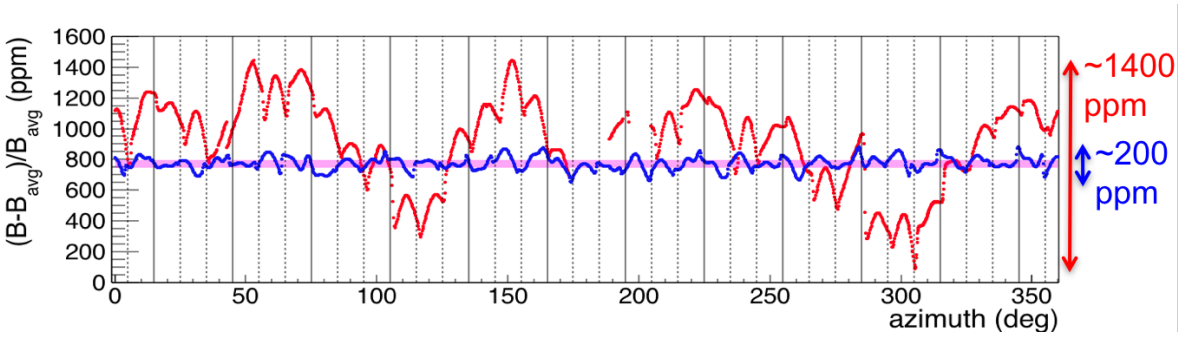

Figure 3. Azimuthal variation of the 1.45 T magnetic field of the storage ring during the shimming program. The red curve indicates the field variation in October 2015 and the blue curve indicates the field variations in June 2016. The shimming program untimately achieved a uniformity of ±50 ppm (the pink band).

4 Experiment status

The Fermilab muon campus is shown in Fig. 2. A number of existing components of Fermilab's accelerator complex are being reused to deliver fills of polarized, magic momentum muons to the g-2 storage ring. Protons bunches are first accelerated to 8 GeV using the booster ring. These bunches are then dispatched via the recycler ring to the AP0 target facility which is now repurposed as a pion source. Existing transfer lines are tuned to collect the 3.11 GeV/c pions from proton spallation and capture the 3.094 GeV muons from $\pi \rightarrow \mu\nu$ decay. Lastly the recycler ring – now renamed the delivery ring – is used to separate in time the muons from pions and protons with the muons then being directed to the g-2 storage ring via a newly-built transfer line. The design eliminates the prompt "flash" of pions and protons and – based on simulations and measurements – is expected to a yield an incident rate of 5-10×10^4 μ^+ per fill.

The Fermilab g-2 experiment is reusing the 1.45 T superconducting storage ring constructed for the earlier Brookhaven g-2 experiment – *i.e.* involving relocating the storage ring from Upton, NY to Batavia, IL. The move, which included transporting the 15 m-diameter superconducting coils and 650-ton steel yoke, was completed in 2013. The coils were shipped by barge – first south down the Atlantic coast and north up the Mississippi river – on a one-month, 3200-mile journey. The reassembly of the storage ring in the experimental hall of the newly constructed MC-1 building was completed in 2014. Two major milestones – cooling-down the superconducting coils and powering-up the main magnet – were achieved in 2015.

During the period 2015-16 the meticulous process of shimming the ring magnet to reach the required uniformity of magnetic field was carried out (see Fig. 3). This interative procedure progressed from the coarse adjustment of large pole pieces to the fine adjustment of tiny shimming wedges and greatly benefited from modern real-time measurement of field strengths versus shimming adjustments. Ultimately, the procedure led to a ±50 ppm field uniformity – about a four-fold improvement in the field uniformity over the BNL experiment.

In addition to the 5172 A main magnet for the 1.45 T magnetic field the storage ring incorporates a superconducting inflector, three pulsed kickers, and four electrostatic quadrupoles. The superconducting inflector and pulsed kickers are together responsible for channeling the injected muons onto the central orbit of the storage ring. The electrostatic quadrupoles provide the vertical confinement of stored muons.

Over the past year various new or refurbished detector packages have been installed. These packages include the twenty four electromagnetic calorimeters and the associated laser calibration system for the precision measurement of the positron time and energy distribution as well as in-vacuum straw trackers for positron tracking and in-vacuum scintillating fibers for muon tracking. A further detector package – comprising a plastic Cerenkov counter and scintillating fiber arrays – was installed to provide time and profile measurements of the beam upstream of the superconducting inflector. The full assembly of the muon storage ring and various detector packages are shown in Fig. 4.

Each calorimeter comprises a 6×9 segmented array of $2.5 \times 2.5 \times 14$ cm^3 PbF_2 crystals [14, 15]. The Cerenkov light from each crystal is detected by commercial silicon photomultipliers (SiPMs), amplified by custom charge-sensitive amplifiers, and digitized by custom, 12-bit, 800 MSPS waveform digitizers. The continuously digitized traces from every crystal of every calorimeter are readout and processed by a 20 GB/s, 100 TFlop data readout and real-time processing system.

The first engineering run of the muon beam, storage ring and various detector systems was conducted in June, 2017. On May, 27 the first signals from a fill were recorded by the electromagnetic calorimeters and the straw trackers. On June, 7 the first evidence of "many-turn" storage of a fill was recorded by the electromagnetic calorimeters and the in-vacuum scintillating fibers. By June, 10 the first positron time distribution or so-called "wiggle plot" showing the time-dilated lifetime $\gamma\tau_\mu$ and anomalous precession frequency ω_a was reconstructed from the high energy positron hits in the electromagnetic calorimeters (see Fig. 5).

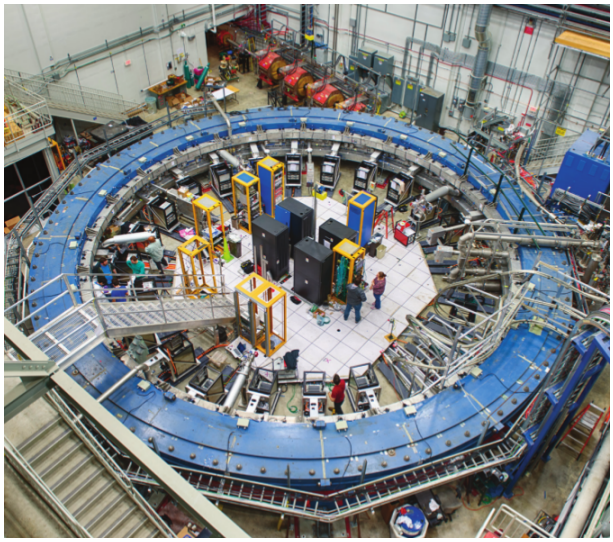

Figure 4. The 7.1 m radius, 1.45 T field, muon storage. The muons are injected at the top-left of the storage ring and the positrons are detected by the twenty four calorimeters abutting the ring's inner circumference.

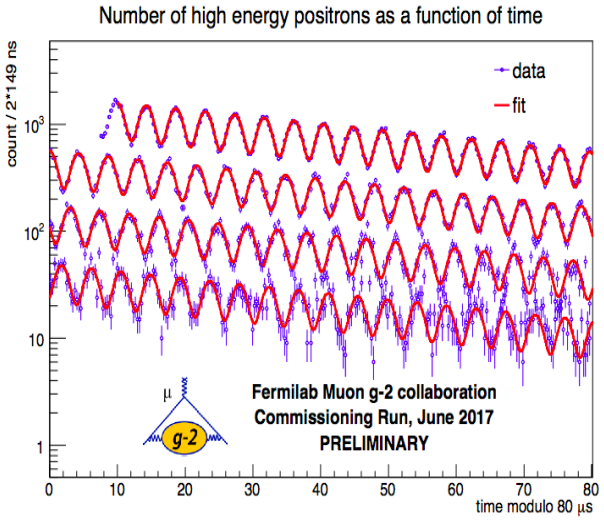

Figure 5. The wiggle plot of the positron time distribution from the June 2017 commissioning run showing the time-dilated muon lifetime $\gamma\tau_\mu$, anomalous precession frequency ω_a, and "best fit" curve.

The run permitted a number of studies of muon delivery and muon injection that currently are informing our efforts to optimize muon storage. Efficient storage requires careful focusing of the beam through the narrow aperture of the inflector, careful timing of the kicker pulsing that displaces particles onto the ring's orbit, and careful optimizing of the electrostatic quadrupoles to provide vertical confinement and avoid beam resonances. The run represented a major milestone in advancing g-2 to data-taking.

5 Experiment future

The goal of determining a_μ to 140 parts-per-billion precision requires improved measurements of the muon anomalous frequency ω_a and the proton Lamor frequency $\overline{\omega}_p$ in comparison to the Brookhaven experiment.

Concerning $\overline{\omega}_p$, we require a roughly three-fold reduction in systematic uncertainties from 170 ppb in the Brookhaven experiment to 70 ppb in the Fermilab experiment. This frequency is a weighted average over the muon azimuthal and transverse distributions in the storage ring. Better determinations of the stored muon distribution using the new positron tracking detectors and the magnetic field variation using the refurbished NMR trolley – along with aforementioned improvements in the field uniformity from the shimming program – are parts of accomplishing this goal.

Concerning ω_a, we require both a twenty-fold increase in detected positrons and a three-fold reduction in systematic uncertainties in comparision to BNL 821. The new Fermilab muon campus is the keystone in the twenty-fold increase in the positron statistics. The latter is achieved by increasing the fills per second of the storage ring, increasing the muons per fill in the storage ring, and extending running time. At time of writing, the push from the low fill rate, low muon rate, engineering run to high fill rate, high muon rate, production running is new underway.

To achieve the goals for ω_a systematics the collaboration built the new detector, electronics and acquisition system for the ω_a measurement. The system was designed to handle the increased rates at Fermilab and also minimize biases in the extraction of the anomalous frequency ω_a from the positron time distribution. The measurement requires extraordinary stability of the detectors and the electronics over the 700 μs measurement periods following the muon beam injection as the positron rates decrease by about four orders-of-magnitude. Serious concerns include pulse pileup, gain changes and pedestal drifts during the measurement periods.

One part of reducing systematics is the readout electronics and acquisition system that facilitates different approaches to determining ω_a. One category of recorded data – the T-method datset – consists of chopped islands of consecutive samples that are triggered by an above-threshold signal. This dataset is used to construct the time distribution of high energy positrons hits by fitting the individual crystal pulses and clustering into reconstructed positron hits. Another category of recorded data – the Q-method dataset – consists of periodic flushes of fill-summed histograms of the 700 μs contiguous traces of ADC samples. This dataset is used to construct the time distribution of the integrated positron energy without the fitting of individual crystal pulses and clustering into reconstructed positron hits. The two datasets incur different systematic dependencies from pulse pileup, gain changes and pedestal shifts and act as "multiple experiments" for measuring ω_a.

The collaboration is currently beginning a running period from November 2017 through June 2018 with similar periods planned for 2018-19 and 2019-20. Our goals are achieving 1-2× the BNL statistics by summer 2018, 5-

10× the BNL statistics by summer 2019, and 20× the BNL statistics by summer 2020.

6 Acknowledgments

The author would like to thank the organizers of the FCCP2017 workshop for a wonderful meeting. The author would also like to thank his Fermilab muon g-2 collaborators and the finanicial support of the U.S. National Science Foundation grant PHY-1503552.

References

[1] G. W. Bennett *et al.* [Muon G-2 Collaboration], "Final Report of the Muon E821 Anomalous Magnetic Moment Measurement at BNL," Phys. Rev. **D73**, 072003 (2006). [hep-ex/0602035].

[2] J. Grange *et al.* [Muon g-2 Collaboration], "Muon (g-2) Technical Design Report," arXiv:1501.06858 [physics.ins-det].

[3] M. Otani [E34 Collaboration], "Status of the Muon g-2/EDM Experiment at J-PARC (E34)," JPS Conf. Proc. **8**, 025008 (2015).

[4] J. P. Miller, E. de Rafael and B. L. Roberts, "Muon g-2: Review of Theory and Experiment," Rept. Prog. Phys. **70**, 795 (2007).

[5] T. P. Gorringe and D. W. Hertzog, "Precision Muon Physics," Prog. Part. Nucl. Phys. **84**, 73 (2015) [arXiv:1506.01465 [hep-ex]].

[6] K. Hagiwara, A. Keshavarzi, A. D. Martin, D. Nomura and T. Teubner, "g-2 of the muon: status report," Nucl. Part. Phys. Proc. **287-288**, 33 (2017).

[7] M. Davier, A. Hoecker, B. Malaescu and Z. Zhang, "Reevaluation of the hadronic vacuum polarisation contributions to the Standard Model predictions of the muon g-2 and alpha(mZ) using newest hadronic cross-section data," arXiv:1706.09436 [hep-ph].

[8] F. Jegerlehner, "Muon g-2 Theory: the Hadronic Part," arXiv:1705.00263.

[9] M. Davier, A. Hoecker, B. Malaescu and Z. Zhang, "Reevaluation of the Hadronic Contributions to the Muon g-2 and to alpha(MZ)," Eur. Phys. J. **C71**, 1515 (2011). Erratum-ibid. **C72**, 1874 (2012).

[10] K. Hagiwara, R. Liao, A.D. Martin, D. Nomura and T. Teubner, "(g-2)$_\mu$ and alpha(M_Z^2) re-evaluated using new precise data," J. Phys. **G38**, 085003 (2011).

[11] F. Jegerlehner, R. Szafron, "$\rho^0 - \gamma$ mixing in the neutral channel pion form factor F_π^e and its role in comparing e^+e^- with τ spectral functions," Eur. Phys. J. **C71**, 1632 (2011). [arXiv:1101.2872 [hep-ph]].

[12] T. Aoyama, M. Hayakawa, T. Kinoshita and M. Nio, "Tenth-Order QED Contribution to the Electron g-2 and an Improved Value of the Fine Structure Constant," Phys. Rev. Lett. 109 (2012).

[13] C. Gnendiger, D. Stockinger and H. Stockinger-Kim, "The electroweak contributions to $(g-2)_\mu$ after the Higgs boson mass measurement," Phys. Rev. **D88** (2013) 053005.

[14] A. T. Fienberg *et al.*, "Studies of an array of PbF_2 Cherenkov crystals with large-area SiPM readout," Nucl. Instrum. Meth. A **783**, 12 (2015). arXiv:1412.5525 [physics.ins-det]].

[15] J. Kaspar *et al.*, "Design and performance of SiPM-based readout of PbF_2 crystals for high-rate, precision timing applications," JINST **12**, no. 01, P01009 (2017). [arXiv:1611.03180 [physics.ins-det]].